Flow Mechanism of Dilatant Systems. (I) Starch Suspension in Water

Jeong-Hwang Bang, Eung-Ryul Kim and Sang-Joon Hahn

Department of Chemistry, Hanyang University, Seoul 133, Korea

Taikyue Ree

Department of Chemistry, The Korea Advanced Institute of Science and Technology, Seoul 131, Korea

(Received June 16, 1983)

Depending on the range of shear rates, temperatures and concentrations, the potato starch suspension in water behaves as a typical dilatant system. The flow curves of the suspension at various concentrations and temperatures were obtained by using a Couette type rotational viscometer. The flow mechanism of the suspension is explained by a structure model of starch granules in the suspension. Based on the experimental results, a general flow equation for the dilatant system is proposed. By analyzing the temperature dependency of the relaxation time, the activation enthalpy and activation entropy for flow in the starch-water suspension were calculated, the former being about 10 kcal/mol.

Introduction

Many empirical or semi-emprirical approaches have been attempted to represent the flow behavior of shear thickening materials, that is, materials which increase the viscosity as the rate of shear increases. Shear thickening of sand-water mixtures was studied by Reynolds.[1] Reynolds used the term dilatancy to describe the shear thickening phenomena associated with a volume increase. Not all the shear thickening is associated with a volume increase, but the term dilatancy is more broadly used for the materials which increase viscosity with increase of shear rate. A fluid which decreases viscosity with the increase of shear rate is usually called shear thinning. A reversible time-dependent decrease of viscosity upon an increase of shear rate is termed thixotropy. Bauer and Collins[2] have reviewed the history of the use of this term. A reversible time dependent increase in viscosity is also called the negative thixotropy for the dilatancy. As for the flow mechanism of thixotropic system, many studies have been published. However, in the case of dilatant systems, not many theoretical interpretations are available.

Hoffman[3] has studied dilatant viscosity behavior in concentrated suspensions of monosized spheres of polymeric resins. The analysis is carried out on the presumption that the dominant forces leading to the flow instability are the van der Waals-London attraction, electric double layer repulsion and the shear stress between ordered layers of spheres. He has pointed out that the latter two forces are more significant than the first one.

Kanno *et. al.*[4] and Umeya *et. al.*[5] have observed that TiO_2-water suspension behaved as a dilatant system. They have observed that the viscosity of the suspension has shown notable increase with the increases in the concentration as well as in shear rate in the TiO_2-water suspension. Hans *et al.*[6] have observed a strong tendency of dilatancy in the case of vinyl copolymer dispersion systems.

In this paper, we studied the mechanism of dilatant flow of potato starch-water suspension. We present here the experimental results thus far obtained, and the theoretical explanation of the results.

Experimental

Materials. Chemically pure potato starch was a commercial product of Junsei Chemical Co. Japan, and the average granular size was approximately 30μ. Carboxymethyl cellulose (CMC), as a dispersion agent, was obtained by the following procedure: 25 m*l* of 85% methanol, 5m*l* of 3*M* HCl and 5g of sodium CMC (Extra pure, Junsei Co.) were mixed and were stirred for 2 to 3 hours at room temperature, and then the precipitates were washed several times with methanol to remove sodium ions, and dried at room temperature. To minimize the effect of impurities in water on the viscosity of the suspension, water was treated with $KMnO_4$ and $K_2Cr_2O_7$ successively and then distilled.

The suspension of starch was prepared by a following procedure. Pure potato starch, product of Junsei Chemical Co., mixed with CMC was swelled with distilled water for five hours at room temperature. The amount of CMC added was 1% by weight of total suspension. The suspension of a fixed concentration in a 250 m*l* flask was gently shaked for few minutes before running the experiment. This condition was kept throughout our studies to obtain reproducible results.

From a preliminary experiment, we confirmed that the shape of starch granules was gradually changed below pH 2 and above pH 11.5, and was significantly destroyed at 50°C. This is in accord with Radley's observation.[7] So we obtained our flow curves at pH 4.5 and below 40°C. The concentrations of starch were 14, 20, 25 and 30 wt.%.

Apparatus. The apparatus used in this study is a Couette type rotational viscometer.[8] For the study of dilatant flow, a rotational viscometer in which test fluid is sheared between rotating cylinders has advantages over tube viscometers. A sample can be sheared as long as desired so that changes in behaviour with time can be followed. This characteristic is quite significant, since the structures of the fluid system vary with shear in dilatant as well as in thixotropic systems.

The sample fills the annular space between the bob and the cup, which are the essential parts of the viscometer. The cup is rotated by means of a gear system. The shear stress,

produced on the surface of the bob by the suspension being sheared in the annular space, is measured by a transducer. The number of revolutions of the cup per minute (rpm.) is controlled by means of a variable speed transmission which is attached to a motor driving the rotation of the cup. The maximum shear rate chosen in the present work was 880 sec^{-1}. The viscometer provides means for continuously increasing and decreasing the applied rates of shear for making a cycle in 30 seconds.

The shear rate of this equipment is given by

$$\dot{S} = \frac{4\pi n}{60(1-s^2)}$$

Here, n is the rpm of the cup, and s is the ratio of the radii of bob and cup. The value of s was 0.9357.

Experimental Results. The flow curves, shear rate $\dot{S}$ vs shear stress f, obtained for the starch-water suspension of various concentrations of starch at 20, 25, 30 and 40 °C are shown in Figures 1, 2, 3 and 4.

From these figures one notes the general feature that the shear rate decreases with increasing shear stress, *i.e.*, a dilatancy. One also notes that (i) the larger $\dot{S}$, the smaller the concentration at a given f and at a constant temperature; and (ii) the larger $\dot{S}$, the higher temperature for a suspension.

Theory

The authors assume that in the starch-water suspension there exist entangled scaffold structure. Dilatancy is often observed in the suspensions where particles interact each other electrostatically or by van der Waals' force, thus forming scaffolding structures. The applied shear stress will reinforce the system to form densly scaffolded entangled structure which makes flow harder. If the external disturbance is removed, the system recovers its original structure.

Thus, the transition, disentanglement (D)⟶ entanglement (E), causes dilatancy of the suspension.

The flow equation of a system, which contains Newtonian and non-Newtonian type flow units is represented by Eq. (1):[9]

$$f=\frac{X_1\beta_1}{\alpha_1}\dot{S}+\frac{X_2}{\alpha_2}\sinh^{-1}\beta_2\dot{S} \quad (1)$$

Here, $1/\alpha_1$ and $1/\beta_1$ are the intrinsic shear stress and

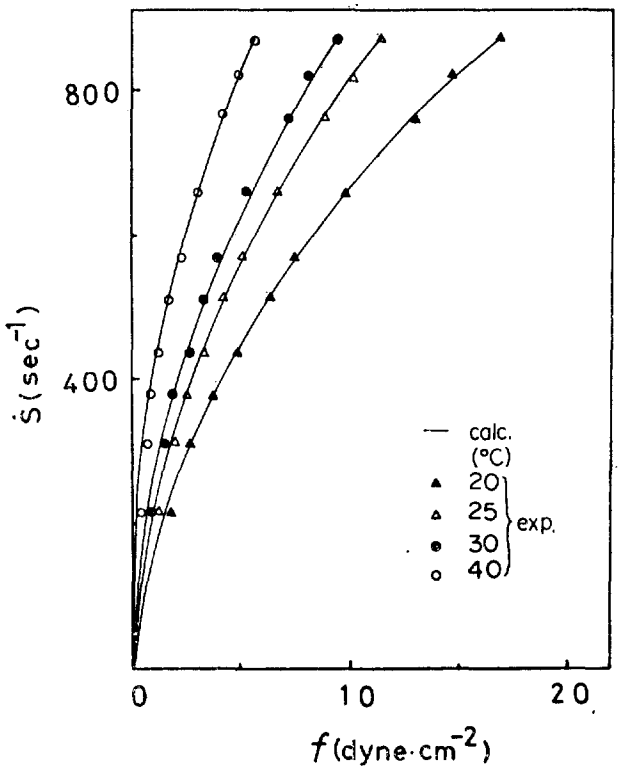

Figure 1. Flow curves of 14 wt.% starch-water suspension at various temperatures. $\dot{S}$=rate of sheer, f=sheer stress.

Figure 3. Flow curves of 25 wt.% starch-water suspension at various temperatures. $\dot{S}$=rate of sheer, f=sheer stress.

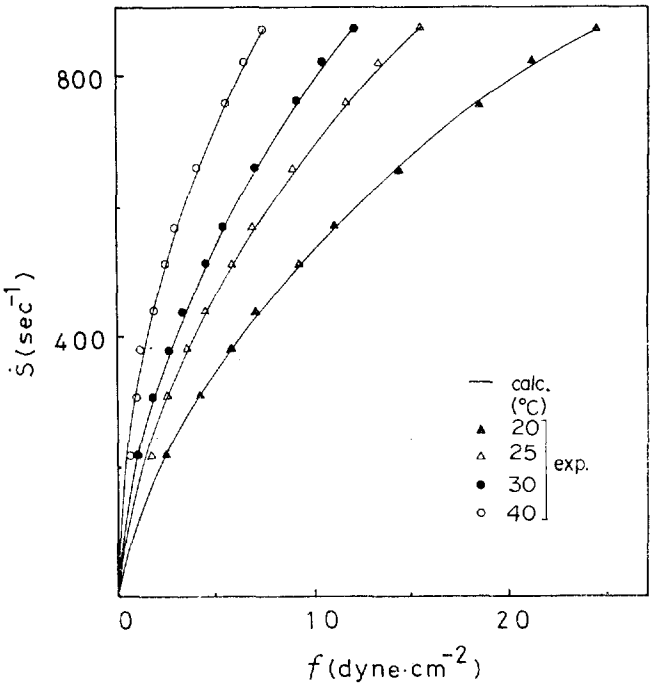

Figure 2. Flow curves of 20 wt.% starch-water suspension at various temperatures. $\dot{S}$=rate of sheer, f=sheer stress.

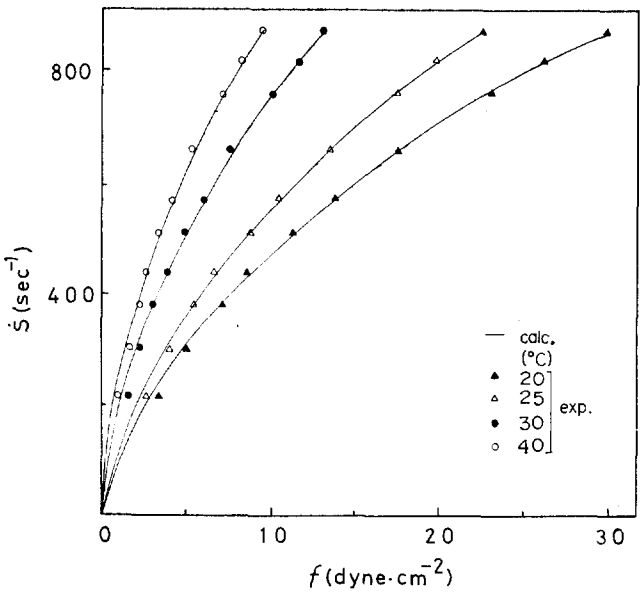

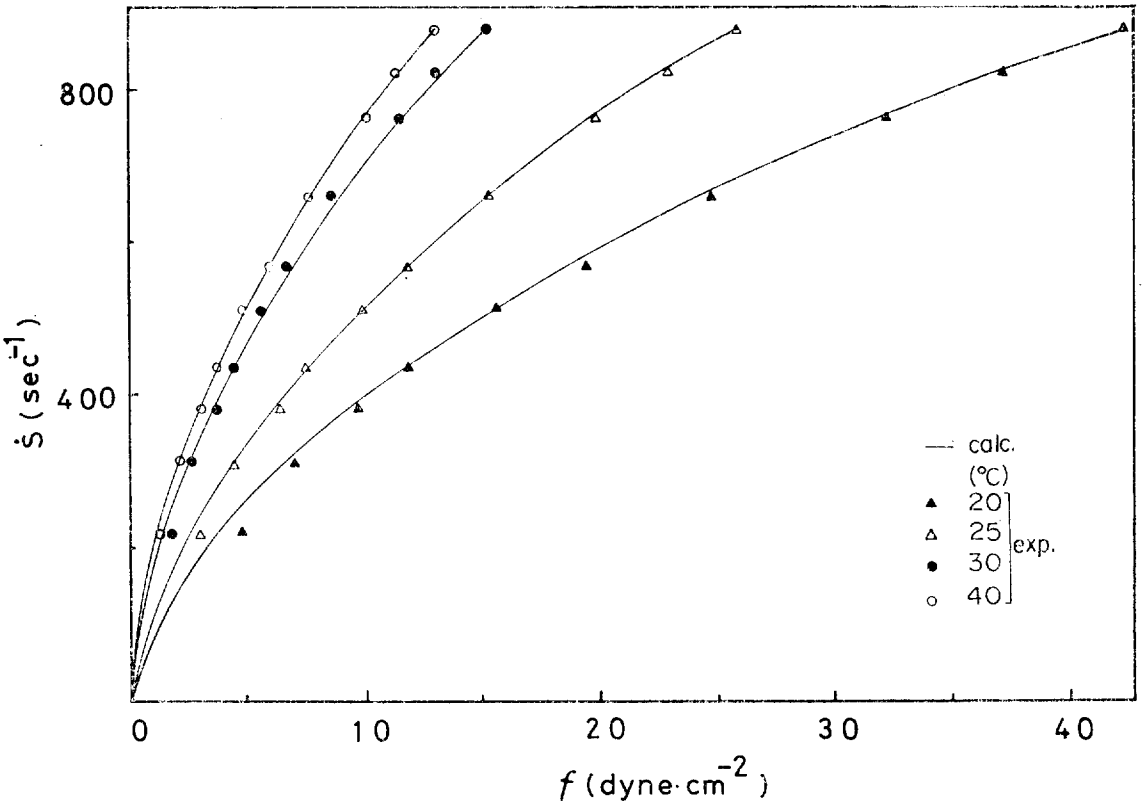

Figure 4. Flow curves of 30 wt.% starch–water suspension at various temperatures. S=rate of sheer, f=sheer strees.

the intrinsic shear rate (β being proportional to the relaxation time) for the Newtonian unit, respectively, and $1/\alpha_2$ and $1/\beta_2$ are the corresponding quantities for the non-Newtonian unit. X_i (i = 1 or 2) is the fraction of the area occupied by the i-th kind of flow units. In a dilatant system, the stress portion contributed by the Newtonian units is negligible. Thus we assume that

$$f=\frac{X_2}{\alpha_2}\sin h^{-1}\beta_2\dot{S} \tag{2}$$

Here,

$$\beta_2=\frac{\lambda_1}{2\lambda k'} \tag{2a}$$

where k' is the rate constant for jumping of a flow unit from an equilibrium position to the next equilibrium position.

If external shear stress f is applied to the dilatant system, the transition $D\longrightarrow E$ occurs due to the work done by the shear. Strain energy, ω, is the work needed for the transition, *i. e.*, to form an entangled structure of the molecules or granules, and the newly formed structure stores the energy of ω.

The strain energy is calculated by the following equation:[10]

$$\omega=\int_0^s GS\,dS=G\gamma\dot{S}^2/2k_f{}^2=C\dot{S}^2 \tag{3}$$

Here, G is the shear modulus of the molecule, and s is the molecular displacemet at which the transition occurs, where $s=\gamma\dot{S}/k_f$, γ being a proportionality constant. The latter relation is obtained from the assumption that the molecular or granular displacement per unit time forced by the shear stress is directly proportional to the shear rate.

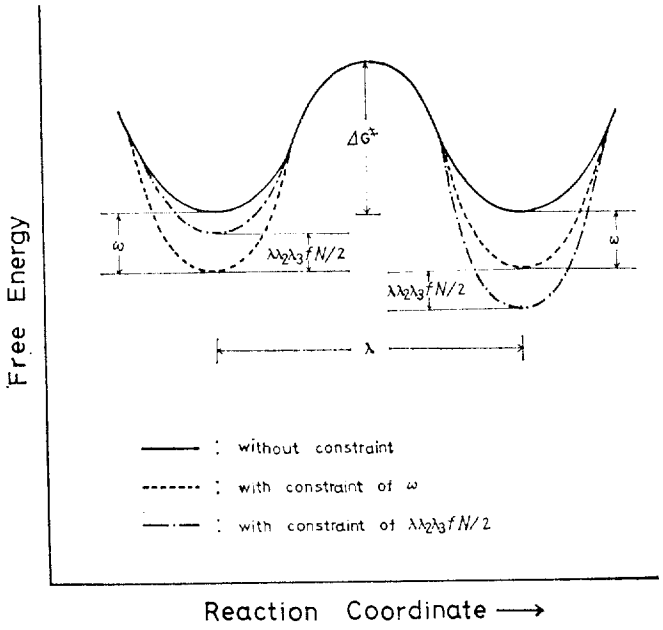

Figure 5. Activation free energy curves. Full curve is for the curve when there is no constraint; dotted curve is for the curve when there is ω constraint, dash and dot curve is for the case where the constraint $\lambda\lambda_2\lambda_3\,fN/2$ is applied to the reinforced structure by a stress, $\lambda\lambda_2\lambda_3/2\,kT$ being equal to α_i in Eq. (1).

In the flow process which is simultaneously accompanied by the transition, the activation free energy of flow is increased by the amount of strain energy ω. Thus, the rate constant k' becomes,

$$k'=\frac{kT}{h}\exp\left[-\left(\frac{\Delta G^{\ddagger}+C\dot{S}^2}{RT}\right)\right]$$
$$=k_0\exp\left(\frac{-C\dot{S}^2}{RT}\right) \tag{4}$$

where, k_0 is the rate constant for the flow unit when there is no constraint. Here the free energy diagram shown in Figure 5 was assumed for the jumping process, *i.e.*, the energy of the activation for flow is increased by ω compared to that when there is no constraint. This is natural since the flow becomes harder by a shear stress, *i.e.*, the energy of the activation is increased by the forced entanglement. Thus, from Eq. (2a), one obtains,

$$\beta_2=(\beta_2)_0 \exp\frac{C\dot{S}^2}{RT} \tag{4a}$$

where

$$(\beta_2)_0\equiv\frac{\lambda_1}{2\lambda k_0}=\frac{\lambda_1}{2\lambda}\frac{h}{kT}\exp\frac{\Delta G^{\ddagger}}{RT} \tag{4b}$$

By substituting Eq. (4a) into (2), one obtains the flow equation:

$$f=\frac{X_2}{\alpha_2}\sinh^{-1}\left[(\beta_2)_0\dot{S}\exp\frac{C\dot{S}^2}{RT}\right] \tag{5}$$

Analysis of the Results

Flow Parameters. The approximation $\sinh X \simeq \ln 2X$, (for $X \gg 1$) is applied to Eq. (5), and one obtains the following equation:

$$\begin{aligned} f&=\frac{X_2}{\alpha_2}\ln\left[2(\beta_2)_0\dot{S}\exp\frac{C\dot{S}^2}{RT}\right] \\ &=\frac{X_2}{\alpha_2}\left[\ln(\beta_2)_0+\ln(2\dot{S})+\frac{C\dot{S}^2}{RT}\right] \end{aligned} \tag{6}$$

By applying Eq. (6) to an experimental flow curve, the unknown parameters, X_2/α_2, $(\beta_2)_0$ and C are obtained. The results are summarized in Table 1.

These parameters were substituted to Eq. (5), and the experimental flow curves were reproduced. The results are shown in Figures 1, 2, 3 and 4 by full curves. One notes that the agreement between theory and experiment is very good.

TABLE 1: The Values of $(\beta)_0$, X_2/α_2 and C

Concentration (wt. %)		14	20	25	30
20 °C	$(\beta_2)_0 10^3$	4.009	5.674	5.782	6.670
	X_2/α_2	0.833	1.104	1.113	1.125
	$C\cdot 10^2$	1.373	1.498	1.872	2.682
25 °C	$(\beta_2)_0 10^3$	3.755	4.326	5.583	6.013
	X_2/α_2	0.721	0.935	1.074	1.107
	$C\cdot 10^2$	1.067	1.097	1.449	1.627
30 °C	$(\beta_2)_0 10^3$	2.553	2.766	3.102	3.987
	X_2/α_2	0.649	0.768	0.802	0.846
	$C\cdot 10^2$	1.013	1.101	1.145	1.246
40 °C	$(\beta_2)_0 10^3$	0.846	1.352	2.347	3.658
	X_2/α_2	0.438	0.539	0.636	0.788
	$C\cdot 10^2$	0.977	1.051	1.083	1.188

$(\beta_2)_0$: sec., X_2/α_2: dyne/cm^2, C: cal. sec^2/mol

Activation Enthalpy $\Delta H^{\ddagger}$ for Flow. In Eq. (5), $(\beta_2)_0$ is represented by Eq. (4b).

Thus, one obtains

$$\ln(\beta_2)_0 T=\ln C'+\frac{\Delta G^{\ddagger}}{RT}=\ln C'-\frac{\Delta S^{\ddagger}}{R}+\frac{\Delta H^{\ddagger}}{RT} \tag{7}$$

where C' equals $(\lambda_1/2\lambda)h/k$. From the data of $(\beta_2)_0$ in Table 1, we plotted $\ln (\beta_2)_0 T$ *vs* T^{-1}, and obtained Figure 6. From Eq. (7), the slopes of the straight lines in Figure 6 yield $\Delta H^{\ddagger}$'s which are summarized in Table 2. From the size (about 10 kcal/mol) of $\Delta H^{\ddagger}$, it may be said that hydrogen bonds may play an important role in making scaffold structure in the suspension.

Discussion

Interaction among Starch Granules in Water. In order to consider the flow mechanism of our system in detail, it is advisable to review briefly the structure of starch granules.

Natural starch granules contain amylose usually amounting to about 15 to 30% of the mass per granule. Recently Gruber et al.[11] have studied the potato starch granules. They showed that potato starch granules may consist of a core of crystalline amylose which is surrounded concentrically by a layered shell of amylopectin as shown in Figure 7. The molecules of amylopectin are deposited as fringed folded micells. By their lateral arrangement they form a layer of higher index of refraction. The molecules are bound to their neighbours by hydrogen bonds.

In water, the outer part of amylopection layers of a starch granule is swollen in some degree, and some of amylopectin molecules are extended toward water. Each granule dispersed in water is loosely connected with the neighboring granules by the extended amylopectin molecules. Thus, the starch granules make a three-dimensional scaffold structure.

When shear stress is applied to the suspension system, a granule under consideration is forced to make more bonds with the neighbors, *i. e.*, the disentangled state becomes an entangled one. Thus, the flow becomes harder, *i. e.*, dilatancy appears. The energy required for making the entangled state is the ω, as previously mentioned.

Activation Entropy $\Delta S^{\ddagger}$

In Eq. (4b), we may assume $\lambda \simeq \lambda_1$. Then, we obtain

$$(\beta_2)_0^{(1)}=\frac{h}{2kT}\exp\left[\frac{\Delta H^{\ddagger(1)}-T\Delta S^{\ddagger(1)}}{RT}\right] \tag{8}$$

where the superscript (1) indicates that the quantity belongs to the 20% suspension. By using the data of $(\beta_2)_0^{(i)}$ and $\Delta H^{\ddagger(i)}$ in Tables 1 and 2 for the 20% suspension at 20°C, the $\Delta S^{\ddagger(1)}$

TABLE 2: Activation Enthalpy of Flow

Concentration (wt.%)	Activation enthalpy $\Delta H^{\ddagger}$ (kcal/mol)
14	13.83
20	12.42
25	10.17
30	6.84

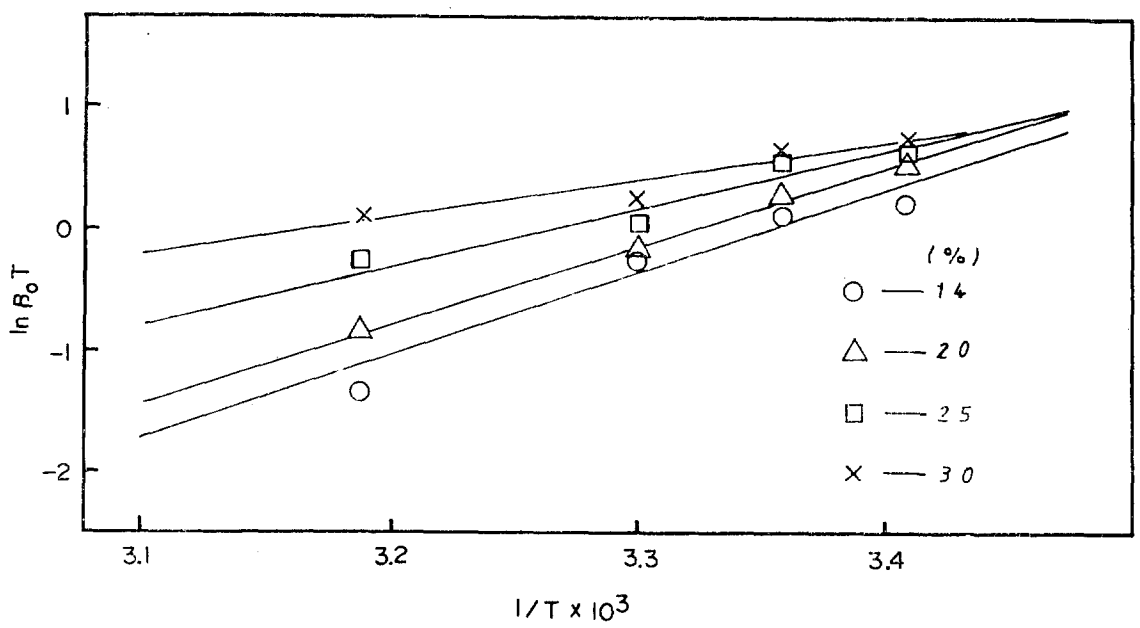

Figure 6. ln $\beta_0 T$ *vs.* $1/T$ for various samples.

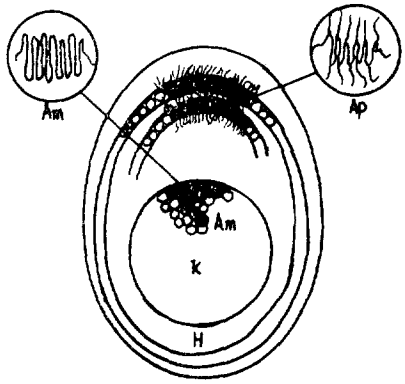

Figure 7. The structure of potato-starch granule. K: core, H: shell, Am: amylose, Ap: amylopectin.

was calculated as $\Delta S^{\ddagger(1)} = -7.06$ eu. By a similar calculation, the $\Delta S^{\ddagger(2)}$ for 30 % suspension at 20 °C was obtained as $\Delta S^{\ddagger(2)} = -26.53$ eu. One notes here that a more concentrated suspension has a more negative $\Delta S^{\ddagger}$ than a less concentrated suspension. The negative $\Delta S^{\ddagger}$ value indicates that the flow unit accompanies a volume contraction in the formation of the activated complx. Thus the fact, $\Delta S^{\ddagger(1)} > \Delta S^{\ddagger(2)}$, shows that in the concentrated suspension, more volume contraction occurs in the concentrated suspension because of the crowded situation in the activation process.

We calculate the activation free energies by using the following equations:

$$\Delta G^{\ddagger(1)} = \Delta H^{\ddagger(1)} - T\Delta S^{\ddagger(1)}$$

and

$$\Delta G^{\ddagger(2)} = \Delta H^{\ddagger(2)} - T\Delta S^{\ddagger(2)}$$

By substituting the values of $\Delta H^{\ddagger(i)}$ (Table 2) and $\Delta S^{\ddagger(i)}$ ($i=1$ or 2) which are known already, the $\Delta G^{\ddagger(i)}$ are obtained as

$$\Delta G^{\ddagger(1)} = 14.49 \text{ kcal} \quad (9)$$

and

$$\Delta G^{\ddagger(2)} = 14.61 \text{ kcal}$$

From Eq. (9) one notes the socalled "compensation effect" occurs in this case. That is, the $\Delta H^{\ddagger(2)}$(=6.48 kcal/mol) for the 30% suspension is considerably smaller than the $\Delta H^{\ddagger(1)}$ (=12.42 kcal/mol) for the 20% sample, because of the $\Delta S^{\ddagger(i)}$ (*i.e.*, $\Delta S^{\ddagger(2)} = -26.53$ eu, $\Delta S^{\ddagger(1)} = -7.06$ eu), however, we obtain the result $\Delta G^{\ddagger(2)} \simeq \Delta G^{\ddagger(1)}$ [see Eq. (9)].

Rates of Shear

In Eq. (5), the rate of shear $\dot{S}$ is given by the following equation:[9]

$$\dot{S} = \frac{\lambda}{\lambda_1} 2 k_0 \exp\left(\frac{-C\dot{S}^2}{RT}\right) \sinh \alpha f \quad (10)$$

In Eq.(5) it may be assumed that $X_2 \simeq 1$.

We assume that $(\lambda/\lambda_1)^{(1)} \simeq (\lambda/\lambda_1)^{(2)}$ and $\alpha^{(1)} \simeq \alpha^{(2)}$. In Eq. (10), $k_0^{(1)} \simeq k_0^{(2)}$ from Eq. (4b), where $\Delta G^{\ddagger(1)} \simeq \Delta G^{\ddagger(2)}$. We note from Figures 2 and 4 that $\dot{S}^{(1)} = 348.6$ sec^{-1} and $\dot{S}^{(2)} = 262.8$ sec^{-1} at 20 °C and $f = 5$ dyne cm^{-2}, *i.e.*, $\dot{S}$ for a dilute suspension is larger than that for a concentrated sample under equal conditions. This fact, which is well known experimentally, is explained by the factor of $\exp(-CS^2/RT)$ in (10) with the aid of the above assumptions. The constants are $C^{(1)} = 1.498 \cdot 10^{-2}$ and $C^{(2)} = 2.682 \cdot 10^{-2}$ cal·sec^2/mol (see Table 1) at 20 °C. If the above assumptions are correct, we obtain,

$$\frac{\dot{S}^{(1)}}{\dot{S}^{(2)}} = \exp\left[\frac{-C^{(1)}(\dot{S}^{(1)})^2 + C^{(2)}(\dot{S}^{(2)})^2}{RT}\right] \quad (11)$$

By using the data of $\dot{S}^{(i)}$ and $C^{(i)}$ mentioned above, we botain the values of the left-hand and the right hand side terms of Eq. (11) are calculated as 1.33 and 1.05, respectively. The discrepancy between the two values may be due to the fact that the assmption is not exactly true. But, we may say that Eq. (11) is approximately correct, consequently our

theory is fairly correct.

Acknowledgement. One of the authers (S.J. Hahn) wishes to acknowledge the Korea Research Center for Theoretical Physics and Chemistry for the financial support of this study.

References

(1) O. Reynolds, "The Structure of Universe," Cambridge University Press, 1903.
(2) W. H. Bauer and E. H. Collins, in "Rheology: Theory and Application," Vol. 4 (edited by F. R. Eirich), P. 423–459. Academic Press. 1967.
(3) R. L. Hoffman, *J. Colloid. Interface Sci.*, **46** (1974).
(4) T. Kanno, M. Wagatsuma and K. Umeya, *Nippon Reoroji*, **4**, 170 (1976).
(5) K. Umeya, T. Kanno and M. Wagatsuma. *Nippon Reoroji*, **4**, 43 (1976).
(6) W. Hans and W. Gerhard, Eur. Pat. Appl. Ep 43, 464 (1982).
(7) J. A. Radley, "Starch and Its Derivatives" (3rd Ed.), P. 90. John Willey & Sons, Inc., New York, 1954.
(8) H. Utsugi, K. Kim, T. Ree and H. Eyring, *Spokesman* (the Journal of National Lubricating Grease Institute), **25**, 125 (1961); A. F. Gabrysh, R. H. Wooley, T. Ree, H. Eyring and C. J. Christensen, Technical Report, Bull. No. 106, Utah Engineering Experiment Station, University of Utah, 1960.
(9) T. Ree and H. Eyring, *J. Appl. Phys.*, **26**, 793, 800 (1955).
(10) S. J. Hahn, T. Ree and H. Eyring, *Ind. Eng. Chem.*, **51**, 856 (1959).
(11) Von E. Gruber, K. John and J. Schurz, *Staerke*, **25**, 109 (1973).

Differential Titrimetric Determination of Bismuth[1]

Q. Won Choi†

Department of Chemistry, Seoul National University, Seoul 151, Korea

H. S. Lim

Hughes Research Institute, CA 91301, U. S. A. (*Received June 22, 1983*)

A precise EDTA titrimetric method involving a weight titration of major portion with solid reagent followed by titration of the remainder with a very dilute standard solution has been developed for the determination of bismuth. When the end point is determined by means of amperometry with a rotating mercury electrode, the error in bismuth analysis is less than 0.01% even when Pb^{2+}, Zn^{2+}, or Cd^{2+} is present. However, copper interferes appreciably and masking with thiourea gives too low results.

It is well know fact that analog measurements by reading a single scale produce results of limited precision. As in differential thermal analysis, weighing with chemical balance, or bridge circuit measurement, if an analog measurement is applied to the difference of an unknown quantity and an accurate quantity close to the quantity to be measured, the precision of the result can be improved darstically. Although similar but not exactly the same principle has been applied in differential spectrophotometry.

In the determination of Te or Se, Barabas and Bennett[2] reduced the major portion of the analyzing constituent first with a measured amount of reducing agent then titrated the remainder with a dilute solution of the same reducing agent, in order to improve the precision of titrimetric procedure. Determination of Co (II) employing weight titration followed by back titration with dilute standard solution of EDTA has been applied in indirect determination of beryllium in order to improve precision.[3] Oxidation of U (IV) with potassium dichromate has been carried out with a precision better than ±0.01% by adding almost stoichiometric amount of the solid reagent and titrating the remainder with a dilute solution.[4]

In the present work, a procedure for differential titration of bismuth with EDTA has been developed. Since high purity bismuth is readily available and the atomic weights involved in the stoichiometric calculations are known to the highest precision, development of a high precision titrimetric procedure appears to be feasible not only for the determination of bismuth but also for standardization of the EDTA solution. Furthermore, the atomic weight of bismuth and the formula weight of EDTA are both large, facilitating precision analytical procedure. Extremely large stability of EDTA complex of bismuth enables the precise determination of the end point. In the present work, a procedure for the differential titration of bismuth with EDTA is desribed.

Experimental

Apparatus. The apparatus has been described previously.[5]

Reagents. High purity (9*N*) bismuth (Nippon Mining Co. Ltd., Lot No. 014-13-785) and disodium salt of EDTA (Fisher, GR grade) are used without further treatment.

Procedure. A weighed amount of bismuth metal is dis-